

THE FOURTH POWER IN THE UNIVERSE

D. D. Jones

September 1973

WP-73-5

Working Papers are not intended for distribution outside of IIASA, and are solely for discussion and information purposes. The views expressed are those of the author, and do not necessarily reflect those of IIASA.

THE FOURTH POWER IN THE UNIVERSE

D.D. Jones

SIZE DISTRIBUTIONS IN NATURE

Introduction

This paper reviews a collection of non-ecological size distributions that have been observed in nature. The range of sizes covers 37 orders of magnitude. Ecologically significant size distributions are reported elsewhere. What can we hope to find in this collection? First we can ask if there are any generalities that exist, and if so, why? In the examples that follow one particular form of distribution is ubiquitous.

What might be the ecological significance of this? First we can ask if these distributions are simply a result of some random statistical process. If not, then what are the specific mechanisms which counterbalance and lead to these distributions? Then we can compare these distributions with those of ecological significance. If the same types appear, then we may have a clue to an explanation. If some other types are found in animal communities, we must look for the special mechanisms that make ecological size distributions different.

Types of Distributions

Size distributions are commonly listed in many different ways. In most cases one method can be easily converted into another. As the examples that follow were taken directly from the literature, there is no uniformity. The details of the transformations are left to the reader's imagination.

Size distributions relate some attribute of an object-class (or a phenomenon) to some characteristic dimension of the object. In most of the examples, the dimension is expressed in units of length. The attribute is commonly the number per unit size interval:

$$n(r) dr = \text{the number with a size} \quad (1) \\ \text{within the increment } r \text{ to } r+dr.$$

Other attributes are volume, mass, surface area, etc. For example, the volume distribution for spheres is

$$v(r) dr = 4/3\pi r^3 n(r) dr, \quad (2)$$

i.e., the volume contributed by the increment dr is the number within dr times the volume of a sphere with radius r .

The size parameter is either a linear dimension (i.e. cm.) or the logarithm of the dimension.

The above distributions are frequency distributions. In many of the examples cumulative distributions are used. The cumulative number

distribution is

$$\begin{aligned} N(r) &= \text{number of objects with a size equal to or less than } r. \\ &= \int_0^r n(r) dr . \end{aligned} \quad (3)$$

Note that

$$\frac{dN(r)}{dr} = n(r) . \quad (4)$$

The cumulative distribution is also expressed as the number with a size greater than a size r .

Two major forms of distributions will be illustrated by the examples that follow. One is the lognormal distribution -- where $n(\log(r))$ is normally distributed about some mean value of $\log(r)$. More will be said about this for specific examples. The other type is the "hyperbolic" distribution:

$$n(r) = kr^{-a} , \quad (5)$$

where k and a are constants of the distribution. This distribution is characterized by a straight line on log-log paper.

As stated, Eq. (5) extends from $r=0$ where there are an infinite number of infinitely small particles to $r=\infty$ where there are no particles. To be physically meaningful the distribution must be truncated at the ends. This truncation can either be characteristic of the natural population of particles or resulting from the method of sampling.

Theory

Some theoretical interest has evolved to explain the consistency of many of the observed distributions. Various mechanisms have been proposed including coagulation, sedimentation, condensation, fragmentation, diffusion, and absorption. Dynamic equilibrium between creation and the differential removal mechanisms lead to certain "self-preserving" or stable size distributions. The exact limiting stable form will depend upon the particular processes. For further reference see: Friedlander, Hurdan, Cadle, Gaudin and Meloy, Gilvarry, Bader, and Mason.

One particular stable form occurs in many situations. This is

$$n(r) = r^{-4}; \quad (6)$$

that is, a graph of $n(r) = dN/dr$ has a slope of minus four on log-log paper. This form is equivalent to the following:

$dN/d \log(r)$	vs.	r	slope = -3
N	vs.	r	slope = 3
N	vs.	vol or mass	slope = 1
dN/dv	vs.	v	slope = -2
dN/dA	vs.	area	slope = -2.5
N	vs.	area	slope = 3.5

Cumulative distributions (N) may have either sign.

An interesting consequence of this distribution is that $dV/d \log(r)$ versus $\log(r)$ is a constant. That is, the volume (or mass) contribution in any log increment is the same. For further discussion see: Friedlander and Pasceri, Pasceri and Friedlander, and Jung.

I. Sizes of particles

What follows is a selective sample of particle size distributions for physical objects in the universe -- starting from atomic dimensions (10^{-10} m) to the universe itself (10^{27} m). The figures follow the text. Full-sized figures are available in the workshop file.

ATOMIC RADII (Figs. 1 and 2)

The cumulative distribution for 43 elements shows a sharp discontinuity at about 1.2×10^{-10} m. in Fig. 1. Figure 2 shows a similar distribution for crystalline ionic radii for 87 elements. An explanation was not found. The discontinuity or "knee" is indicative of a change in "process" occurring.

SMALL PARTICLES (Figs. 3 - 10)

A lot of statistical work has been done on particles in the micron size range. Figure 3 shows typical size distribution of atmospheric aerosols. Figure 4 applies to stratospheric aerosols. Below 0.1 micron particles are eliminated by coagulation due to Brownian motion. The lower limit of natural aerosols is about 5×10^{-3} microns. Above 20 microns particles are rapidly eliminated by gravitational settling. Figures 5 and 6 are the frequency and cumulative distributions of particles in urban air.

Frequently atmospheric particles are plotted on lognormal paper (Figs. 7 and 8). Lognormal and log-log cumulative plots are not easily related; however, the frequency plots are qualitatively similar. If a lognormal distribution is plotted on Fig. 3, the result is a parabola which is similar in form to the natural distributions. Also note that in all of the plots of Fig. 8, the data points deviate from the straight line in a systematic "S-shaped" manner. This form is found when a truncated distribution, like Eq. (5), is plotted on lognormal paper.

Figure 9 shows the distribution of fine Arizona road dust. Figure 10 shows the size distribution resulting from the fracture of brittle solids. (An animal population analogy to this example should be familiar to all ecologists.)

RAIN DROPS (Figs. 11 and 12)

In-cloud rain droplets are shown in Fig. 11; the form appears to be exponential rather than hyperbolic (it is a linear size scale). Figure 11a is a frequency distribution. Figure 12 applies to falling drops.

SILT, SAND AND GRAVEL (Figs. 13 and 14)

A sample for suspended silt in a B.C. stream is shown on a lognormal plot in Fig. 13. Sand and gravel sizes are shown in Fig. 14. (Plots courtesy of Art Tautz)

LUNAR SURFACE MATERIALS

Meloy and O'Keefe discuss the early Surveyor I photographs where the visible particles were governed by the equation

$$N(r) = N_0 r^{-m} \quad (7)$$

with $m = 1.77$.

METEORITES (Fig. 15)

The size distribution of extraterrestrial influx (at a rate of 100-1000 tons/day) is shown in Figure 15. The slope of the large particles is about -1.0. When this is converted from a cumulative mass distribution to dN/dr , the slope becomes -4.0 again.

ASTEROIDS (Fig. 16)

The size distribution of asteroids appears to be in a transition from an original gaussian to a hyperbolic form (Fig. 16).

PLANETS AND SATELLITES (Fig. 17)

The distribution of planets and satellites in the solar system do not fit a hyperbolic form. Both groups combine into a uniform collection, however.

COMETS (Fig. 18)

The size distribution of comets was not easy to find. Instead, the distribution of orbit sizes is shown in Fig. 18. The discontinuity at 1 a.v. (earth-sun distance) is attributed to a reduced probability of observation for large orbits.

STARS (Fig. 19)

The visual magnitude of stars in the solar neighborhood is shown in Fig. 19. The magnitude (a linear scale) is related to the log of the radius.

PLANETARY NEBULAE (Fig. 20)

Planetary nebulae are shells of ejected gas expanding about certain extremely hot stars. The data correspond to our galaxy only. The size measure is the angular diameter, which is a function of true diameter and distance from earth.

GALAXIES (Fig. 19)

The visual magnitude of galaxies is related to the cumulative frequency by

$$\log N = 0.5m - 7.2 \quad (8)$$

This equation is plotted on Fig. 19.

THE COSMOS (Fig. 21)

This Figure is redrawn from an intriguing paper by Albert Wilson on the hierarchical structure of the Universe. The regions of sizes and masses of various "particles" are shown. The gaps in the size ranges are apparently very real and numerically related to various fundamental atomic, electromagnetic, and gravitational parameters.

II. Geographical Features

LAKES (Fig. 22)

The areas of natural fresh-water lakes are shown in Fig. 22. For lakes in the U.S. the distribution is hyperbolic if the Great Lakes are excluded. The lakes of the world have an upper size cut-off because of the limitation imposed by continent size.

RIVERS (Fig. 23)

The major rivers of the world show a similar limitation at the upper end.

MOON AND MARS CRATERS (Fig. 24 - 26)

The cumulative size distribution of maria moon craters is shown in Figure 24. The distributions of moon craters and meteorites are superimposed in Fig. 25. Mars craters estimated from early Mariner flights are in Fig. 26.

ATMOSPHERIC TURBULENCE (Fig. 27)

Atmospheric turbulence can be resolved into distributions of various sized "eddies". Two examples for clear air turbulence are shown in Fig. 27.

ATOMIC ABUNDANCES (Fig. 28)

The abundance of the elements in the earth's crust is shown in Fig. 28. The "size" in this case is the extent of concentration in parts per million.

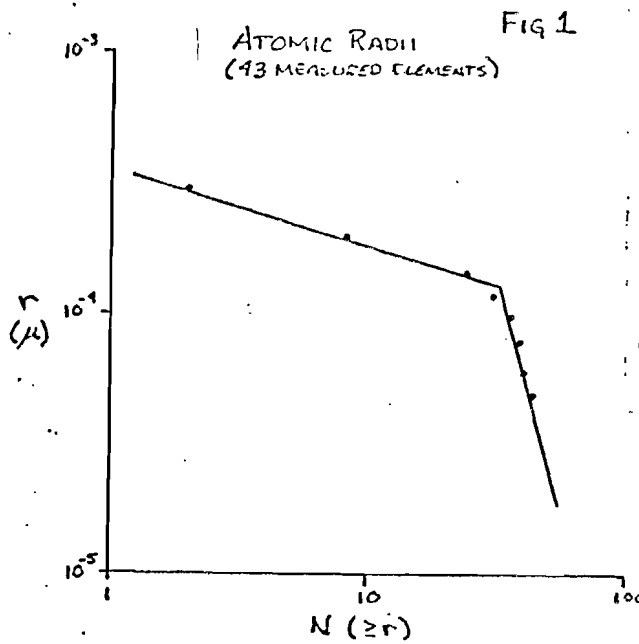
III. Social Phenomena

CITY SIZES (Fig. 29)

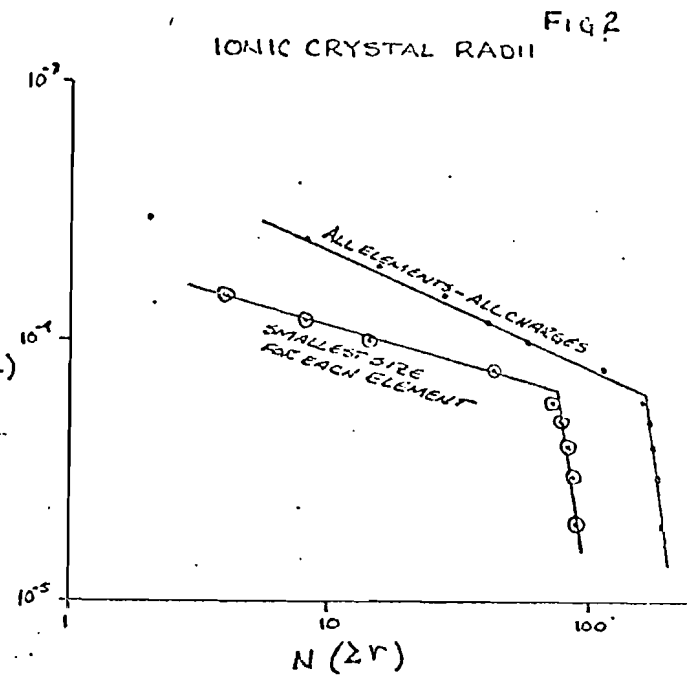
The cumulative distribution of U.S. cities in 1910 and 1960 is shown in Fig. 29.

COLONIES (Figs. 30 and 31)

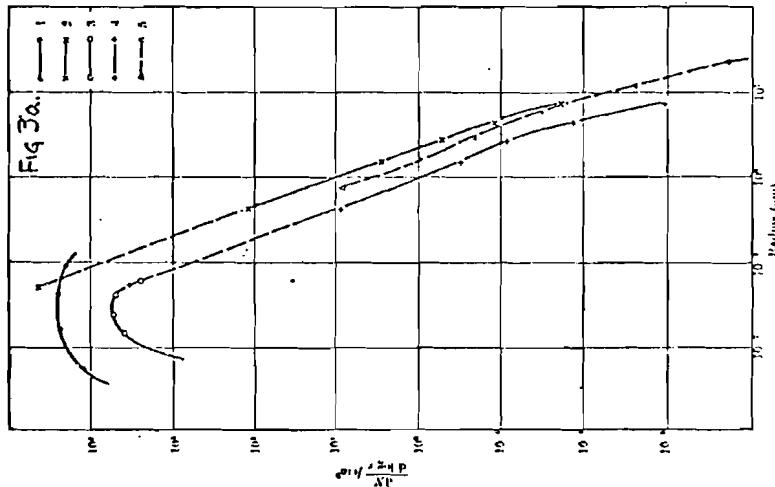
The distribution of mealy-bugs in colonies is shown in Fig. 30. The relationship is not clear from the graph. Williams concluded that the colonies were distributed normally on \log_3 intervals. The population size of pods on cocoa trees is shown in Fig. 31 -- the shape is similar to that of Fig. 30.



SOURCE: C.W. ALLEN, ASTROPHYSICAL QUANTITIES

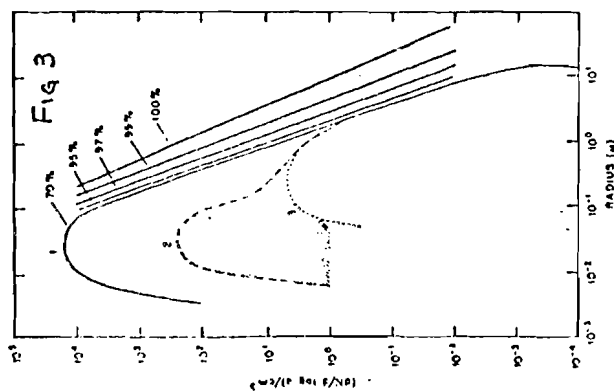


SOURCE: HANDBOOK OF CHEMISTRY AND PHYSICS (1970)

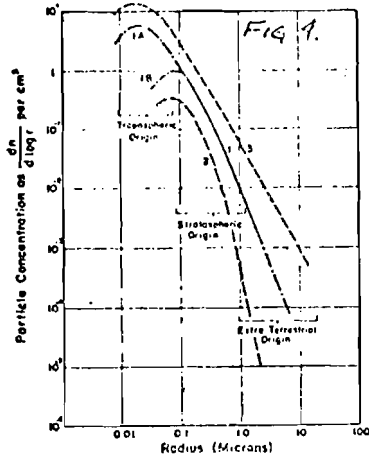


Complete size distributions of natural aerosols, average data. Frankfort curves 1, 2, and 6. Curve 1: ion counts converted to nuclei number. Curve 2: data from impactors. The point below 0.1 μm radius was obtained from the total atmospheric number under the assumption that the radius interval of the diffusion nuclei is $\Delta \log r = 1.0$. Curve 3: average wet-dustion data over a period of 11 days. Curves 1, 2, and 5 are not similar. Zippert, 2000 nuclei above m.s.l.; curves 3 and 4 correspond to curves 1 and 2 for Frankfurt and were obtained at approximately the same time. The dashed curves between 5×10^{-1} μm and 1×10^{-1} μm are interpolated. (From Jung, 1968)

REPRODUCED FROM MASON



Model size distributions for atmospheric aerosols. Curve 1 represents values over a continent, curve 2, over an ocean (the part of this curve below 1 μm is estimated), and curve 3, sea-spray component of the maritime aerosol. The hatched area between curves 2 and 3 represents the non-sea-spray component over the ocean. The straight lines indicate the shift of the continental, the radius-number distribution curve due to particle growth by humidity for mixed particles of about 20% highly material. (From C. K. Fung, in: *Atmospheric Aerosols*, p. 124, Academic Press Inc., New York, 1963)



Average size distribution for stratospheric aerosols. Curve 1A is for the lower stratosphere and 1B for altitudes above 20 km. Curves 2 and 3 are estimated confidence limits. (Courtesy of the American Meteorological Society)

REPRODUCED FROM CADLE

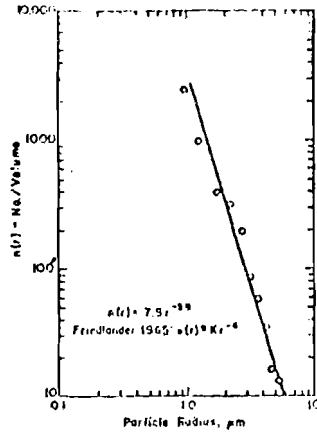


FIG. 5. Size-frequency distribution of r_s (all shapes). FROM STEIN, et al.

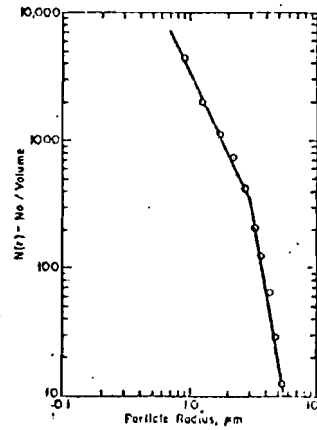
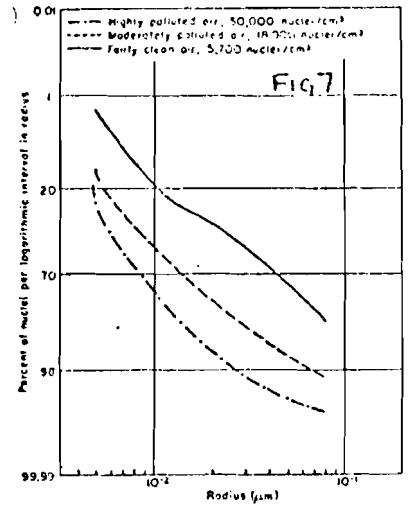
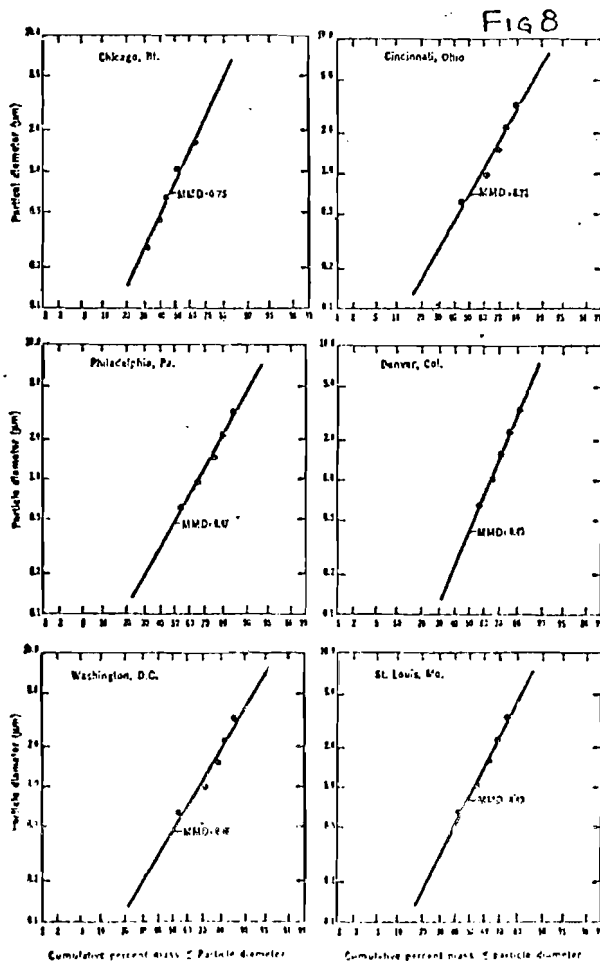


FIG. 6. Integrated size-frequency distribution of r_s (all shapes). FROM STEIN, et al.

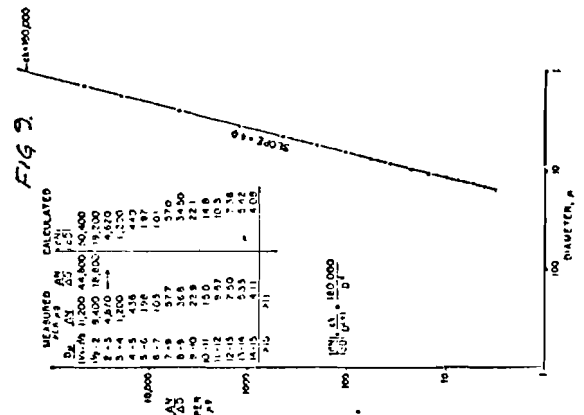


Log-normal plot of typical distributions in clean and polluted air. (From Twomey and Seerynse (78).)



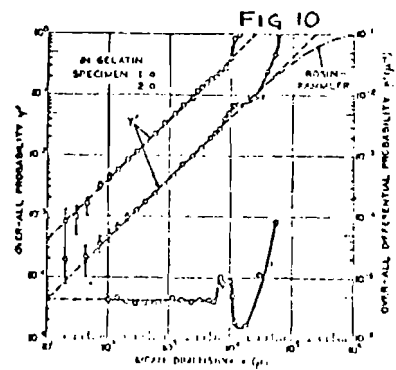
Annual composite particle size distributions for 1970. Chicago, Cincinnati, Philadelphia, Denver, Washington, D.C., and St. Louis. [From Research and Development, June 1972]

REPRODUCED FROM LEE



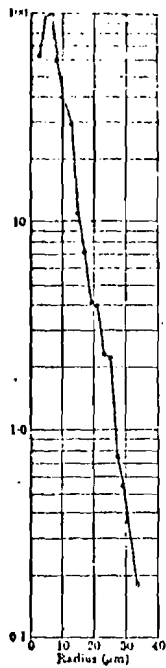
Size distribution of fine Arizona road dust. This illustrates that the combined effects of weathering, grinding by traffic, and wind action can produce an ideal hyperbolic distribution.

FROM BADEE



The probability distribution curves for the overall distributions are based on the measured data and theoretical results for two specimens. The overall differential mobility Y is shown at the top of the overall mobility plot.

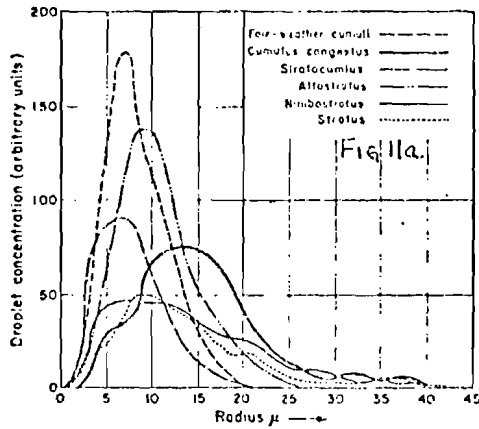
Y IS CUMULATIVE VOLUME



The average droplet-size distribution in fair-weather cumulus. Average liquid-water content 1.0 gm^{-3} ; average droplet concentration 302 cm^{-3} . (From Weickmann and Aufm Kamp (1953).)

REPRODUCED FROM MASON

Fig 11



The droplet-size distributions of various cloud types.

(Courtesy of Springer-Verlag)

REPRODUCED FROM CABLE

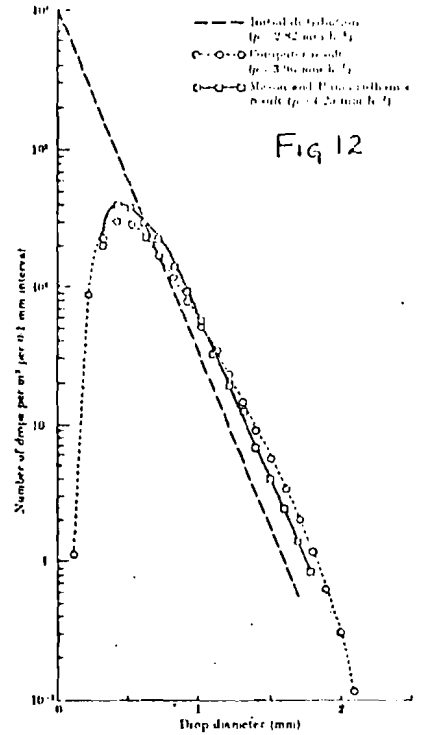


Fig 12

Modification of raindrop size distribution due to coagulation and accretion for a fall of 1 km through a cloud containing 0.2 gm^{-3} of water. --- initial distribution ($p = 2.82 \text{ mm h}^{-1}$), -o-o- Mason and Pruppel's result ($p = 3.06 \text{ mm h}^{-1}$), □-□- Mason and Pruppel's result ($p = 4.25 \text{ mm h}^{-1}$). (From Hardy (1963).)

REPRODUCED FROM MASON

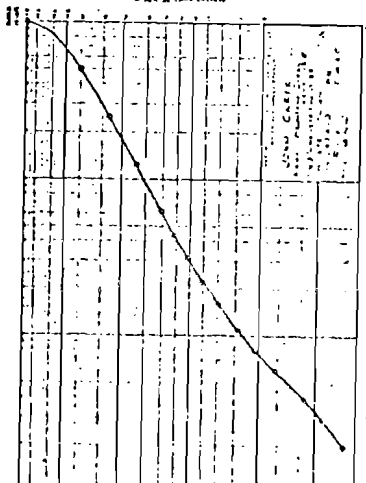
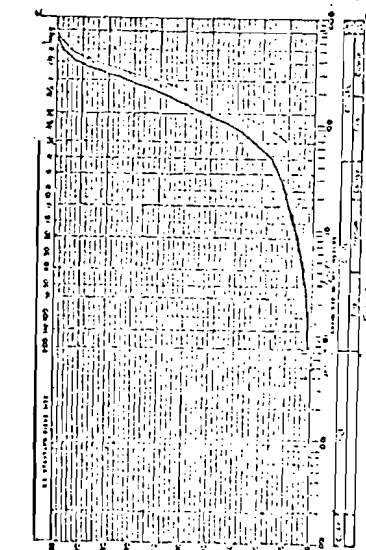
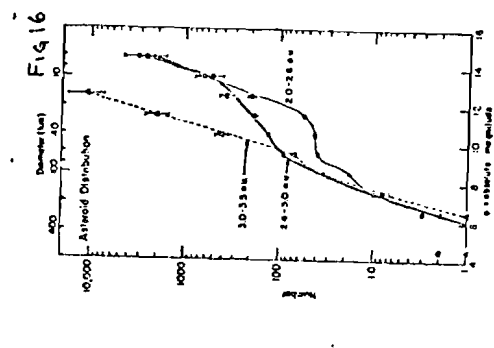


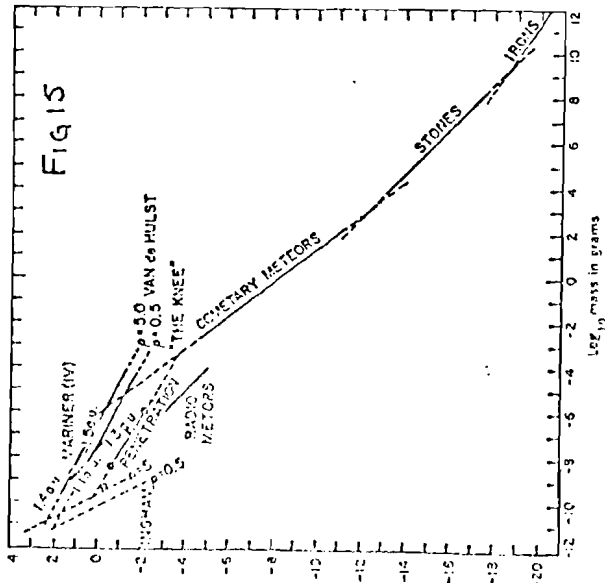
Fig 13

Fig 14



Average size distribution in three zones of the rainforest (Kuijper et al., 1953). Especially in the two inner zones, the curves show a tendency to flatten near $r = 9$. Possibly this marks the transition between an "original" Cumulus distribution and a "fragmentary" distribution.

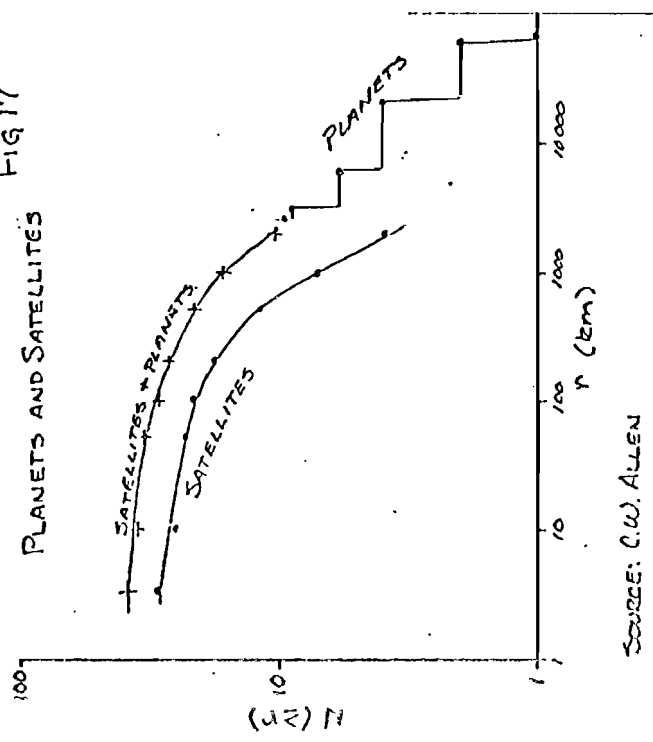
REPRODUCED FROM ANDREWS



Cumulative number index to Earth of extraterrestrial material (number of cm^{-3} per cubic meter per day with mass greater than m (grams)).

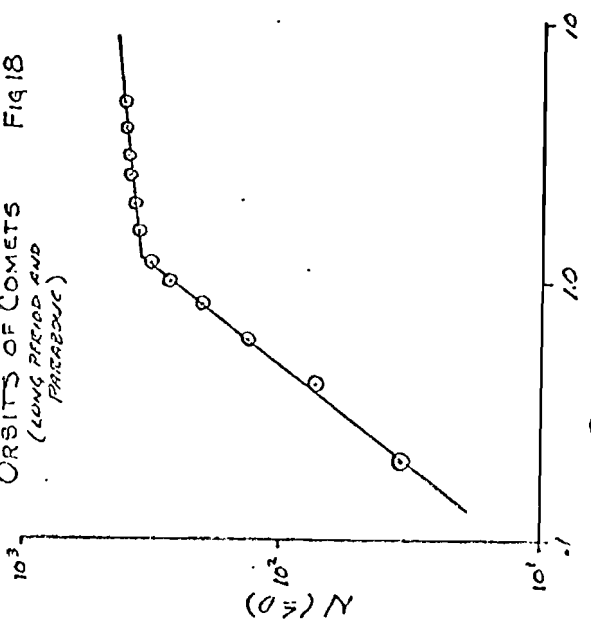
FROM PACEK AND TILDE

FIG 17
PLANETS AND SATELLITES



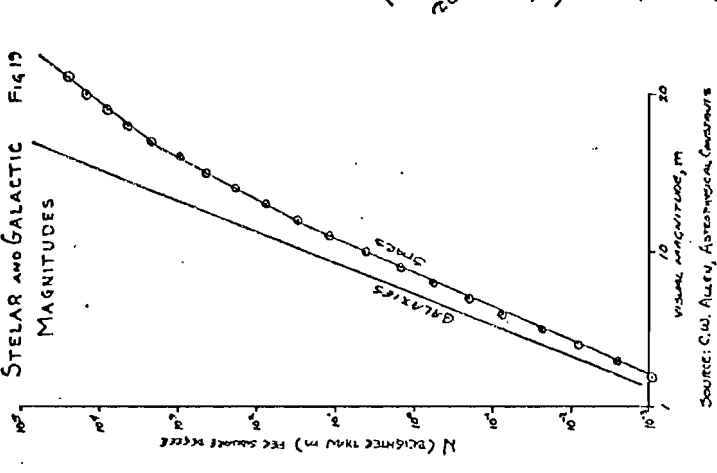
SOURCE: C.W. ALLEN

FIG 18
ORBITS OF COMETS
(LONG PERIOD AND PARABOLIC)



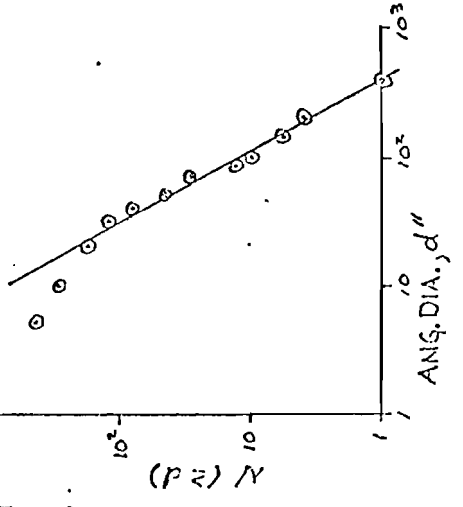
SOURCE: VSEKUSVATENI, S.K., PHYSICAL CHARACTERISTICS OF COMETS

FIG 19
STELLAR AND GALACTIC
MAGNITUDES

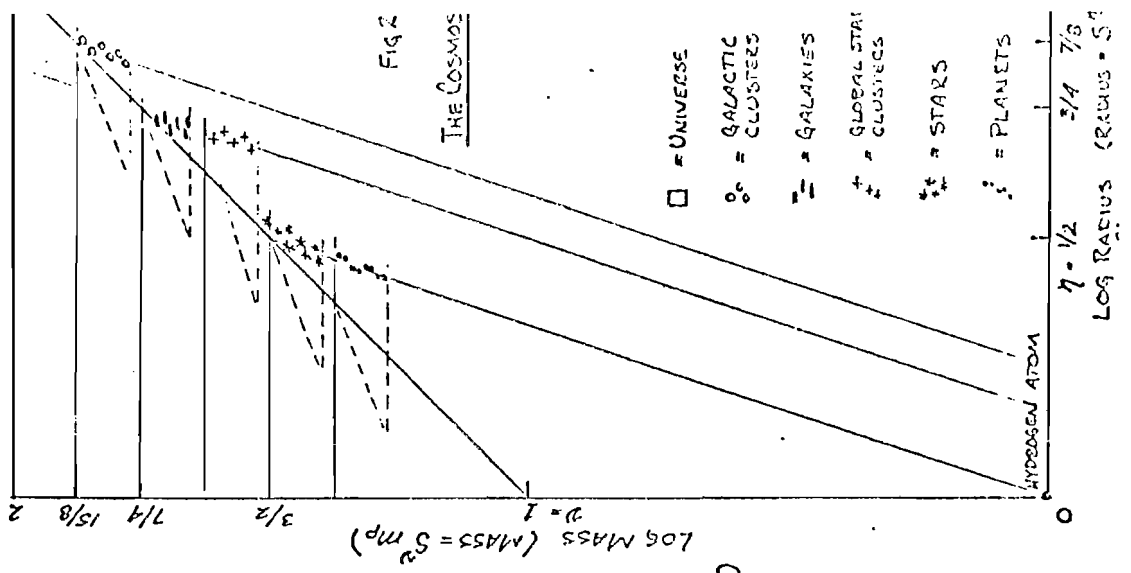


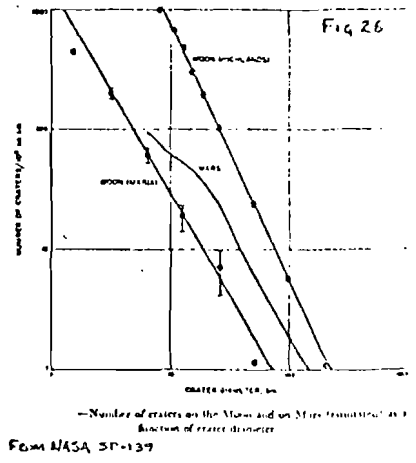
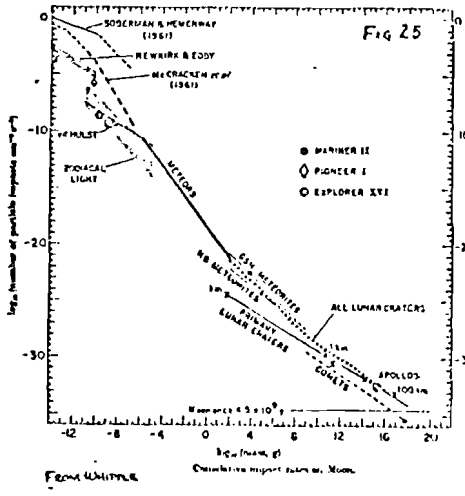
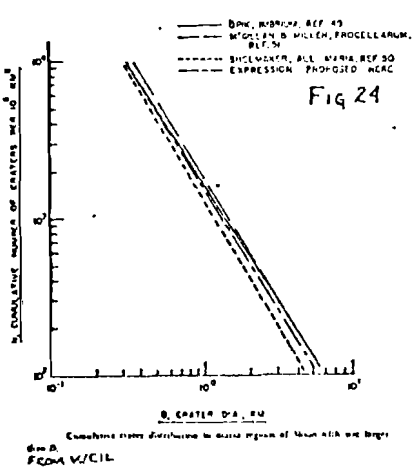
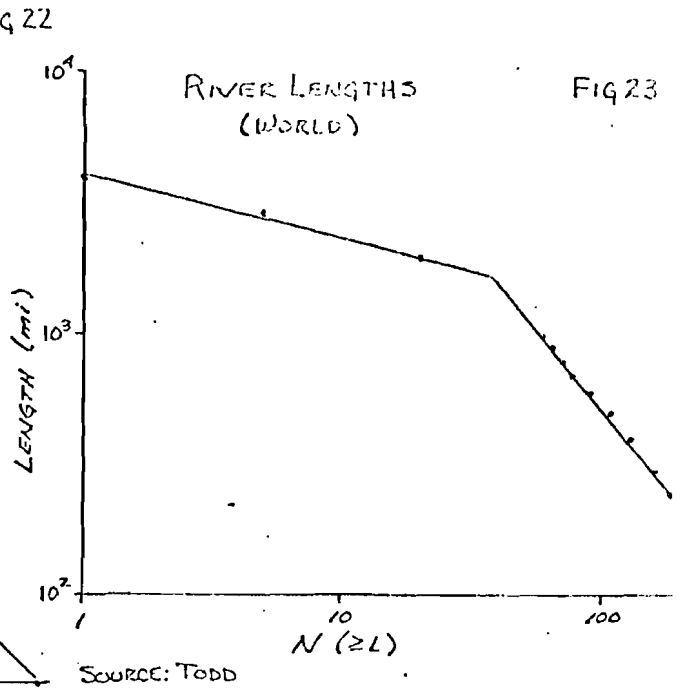
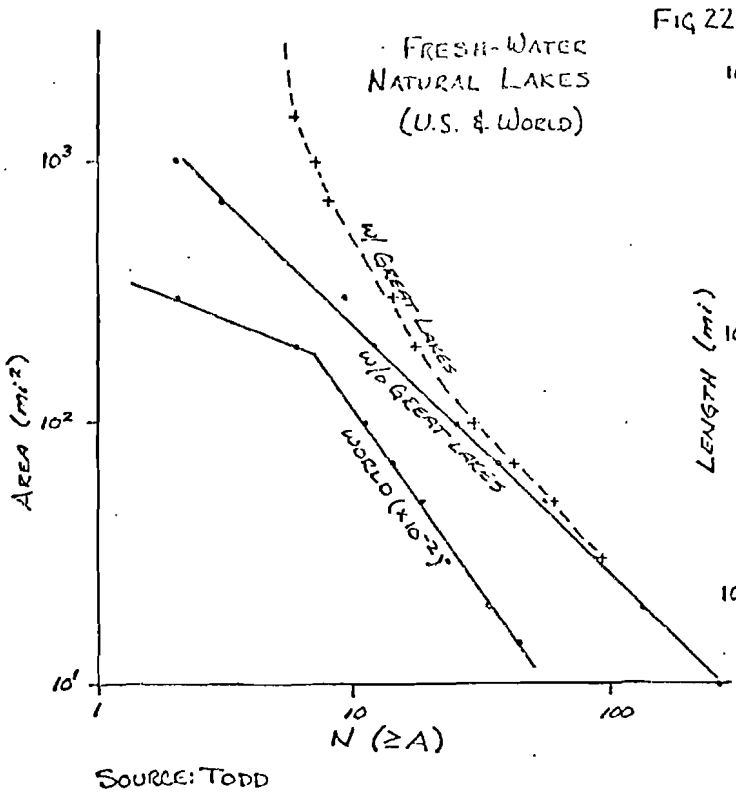
SOURCE: C.W. ALLEN, ASTRONOMICAL QUANTITIES

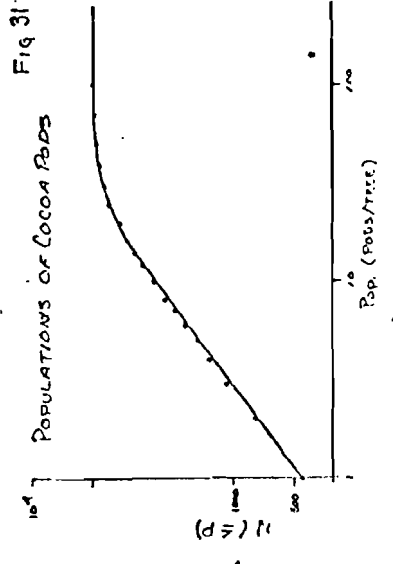
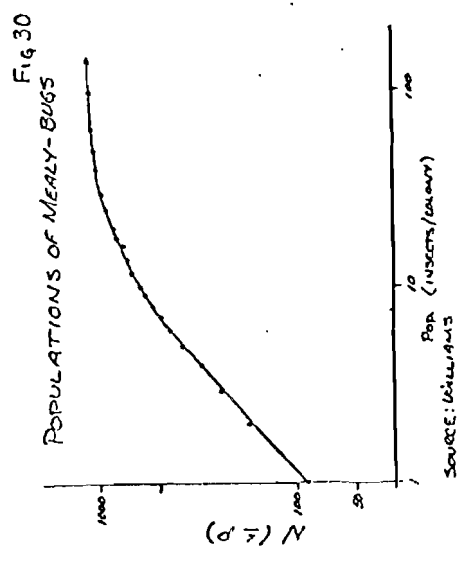
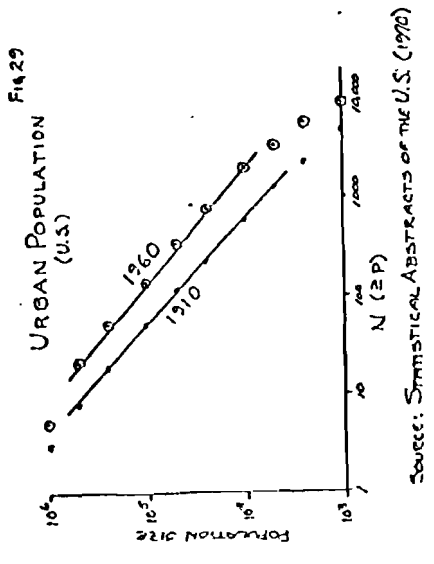
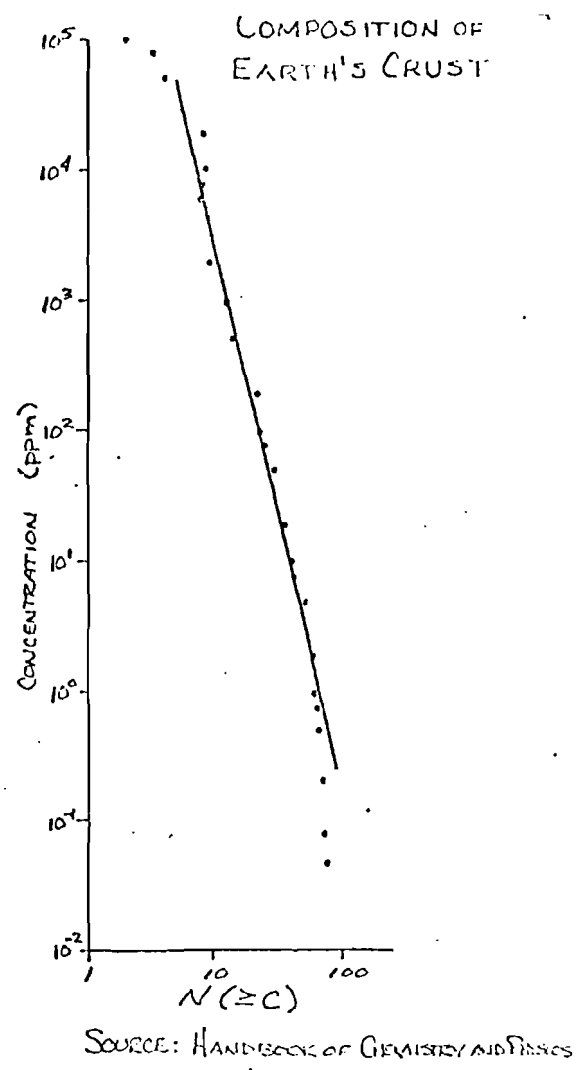
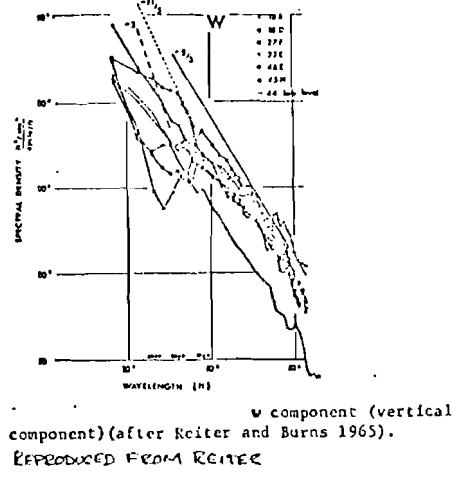
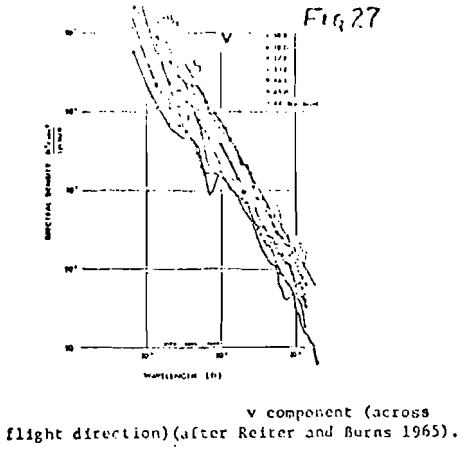
FIG 20
GALACTIC PLANETARY NEBULAE



SOURCE: L. FECK, L. KARGUTSK, CATALOGUE OF GALACTIC PLANETARY NEBULAE







REFERENCES

- Allen, C.W. Astrophysical Quantities, 2nd ed. Athlone Press, London, 1963.
- Anders, E. Icarus 4: 398-408 (1965).
- Bader, H. J. Geophys. Res. 75: 2822-2830 (1970).
- Cadle, R.D. Particles in the Atmosphere and Space. Reinhold, New York, 1966.
- Friedlander, S.K. J. Meteorology 17: 373-374.
- Friedlander, S.K., and R.E. Pasceri. J. Atmospheric Sci. 22: 571-576 (1965).
- Gaudin, A.M., and T.P. Meloy. A.I.M.M.P.E. Mining Trans. 223: 40-43 (1962).
- Gilvarry, J.J. J. Applied Physics 32: 391-399 (1961).
- Gilvarry, J.J., and B.H. Bergstrom. J. Applied Physics 32: 400-410 (1961).
- Handbook of Chemistry and Physics, 52nd ed. Chemical Rubber Publishing Co., Cleveland, 1970 .
- Herdan, G. Small Particle Statistics. Academic Press, New York, 1960.
- Junge, C.E. Air Chemistry and Radioactivity. Academic Press, New York, 1963.
- Lee, R.E. Science 178: 567-575 (1972).
- Mason, B.J. The Physics of Clouds, 2nd ed. Clarendon Press, Oxford, 1971.
- Meloy, T., and J.A. O'Keefe, J. Geophysical Res. 73: 2299-2301 (1968).
- NASA SP-139. Mariner-Mars 1964. Final project report.
- Parkin, D.W., and D. Tilles. Science 159: 936-946 (1968).
- Pasceri, R.E., and S.K. Friedlander. J. Atmospheric Sci. 22: 577-584 (1965).
- Perek, L., and L. Kohoutek. Catalogue of Galactic Planetary Nebulae. Academia Pub. House of Czech. Acad. Sci., Prague, 1967.
- Reiter, E.R. in Pao, Y., and A. Goldberg, Clear Air Turbulence and Its Detection. Plenum Press, New York, 1969.
- Statistical Abstracts of the United States. 1970.
- Stein, F., N.A. Esmen, and M. Corn. Atmospheric Environ. 3: 443-453 (1969).

(References continued)

Todd, D.K. The Water Encyclopedia. Water Information Center, New York, 1970.

Twomey, S., and G.T. Severynse. J. Atmospheric Sci. 21: 558-564 (1964).

Vsekhsvyatskii, S.K. Physical Characteristics of Comets. Israel Sci. Translations, Jerusalem, 1964.

Weil, N.A. Lunar and Planetary Surface Conditions. Academic Press, New York, 1965.

Whipple, F.L. Royal Society London, Proceedings. Ser. A. 296: 304-315 (1967).

Williams, C.B. Patterns in the Balance of Nature. Academic Press, New York, 1964.

Wilson, A. in Whyth, Wilson, and Wilson, Hierarchical Structures. American Elsevier, New York, 1969.